Microporous and Mesoporous Materials 351 (2023) 112483

Contents lists available at ScienceDirect

Microporous and Mesoporous Materials

journal homepage: www.elsevier.com/locate/micromeso

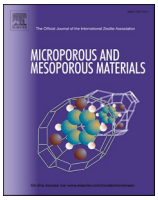

Improving the methyl lactate yield from glucose over Sn–Al-Beta zeolite by catalyst promoters

Atte Aho [a], Narendra Kumar [a], Kari Eränen [a], Robert Lassfolk [b], Päivi Mäki-Arvela [a], Tapio Salmi [a], Markus Peurla [c], Ilari Angervo [d], Jukka Hietala [e], Dmitry Yu. Murzin [a,*]

[a] Laboratory of Industrial Chemistry and Reaction Engineering, Johan Gadolin Process Chemistry Centre, Åbo Akademi University, Åbo, Finland
[b] Instrument Centre, Åbo Akademi University, University of Turku, Åbo, Turku, Finland
[c] Institute of Biomedicine, University of Turku, Finland
[d] Wihuri Physical Laboratory, University of Turku, Finland
[e] Neste Oyj, Research and Development, Porvoo, Finland

A B S T R A C T

Sn–Al-Beta zeolite was prepared through a hydrothermal method and further modified by alkali and alkaline earth (e.g. Sr and Ba) metals not practically altering the textural properties of the catalyst. The catalytic materials were tested in glucose transformation to methyl lactate in a batch reactor at 180 °C allowing to correlate catalytic activity and selectivity with the strength and type of acid sites. The results showed that by suppressing the Brønsted acidity of the modified catalyst with different promoters the yield of methyl lactate can be increased from ca. 20% to over 50%.

1. Introduction

Lactic acid and methyl lactate are important commodity chemicals finding application in the synthesis of polylactic acid, 1,2-propylene glycol, acetaldehyde and 2,3-pentadione. The global market value of lactic acid in 2020 was 3.7 billion USD [1]. This acid can be produced from renewable feedstock such as different sugars, e.g. glucose and xylose as well as from sucrose and inulin in the presence of heterogeneous acid catalysts [2]. Alternatively, fermentation of sugars [3] or glycerol dehydration [4] can be also used for manufacturing lactic acid. Methyl lactate can in turn be produced through esterification of lactic acid or directly from glucose when methanol is used as a solvent in one-pot transformations. If the desired product is lactic acid, methyl lactate can be subsequently converted to lactic acid by hydrolysis during reactive distillation [5].

Sugar transformations to methyl lactate have been intensively studied over different catalysts [6–27]. The transformation of sugars to methyl lactate involves several steps (Scheme 1) requiring acid catalysts, thus both Brønsted and Lewis acidity of potential catalytic materials is very important.

In glucose transformations to methyl lactate (Scheme 1) the reaction starts by isomerization of glucose to fructose. This is followed by the retro-aldol reaction forming dihydroxyacetone and glyceraldehyde, which can be esterified with methanol forming methyl lactate [18].

In the first step glucose is isomerized on Lewis acid sites to fructose, while in the subsequent step the hydroxyl in C4 position is adsorbed on a base site. This promotes cleavage of the C3–C4 bond via a retro-aldol reaction giving a product which is an equilibrium mixture of glyceraldehyde and 1,3-dihydroxyacetone. This intermediate is dehydrated over Lewis acid sites to pyruvaldehyde [19], and thereafter lactic acid is formed through hydration of pyruvaldehyde. This takes place by internal Cannizzaro reaction that involves 1,2-shift of hydrogen. In methanol as a solvent lactic acid is esterified to methyl lactate [21].

Alternatively, pyruvaldehyde reacts with methanol forming pyruvic aldehyde hemiacetal, which undergoes 1,2-shift and esterification [20]. When Brønsted acidity of the catalyst is too high, pyruvic aldehyde dimethyl acetal and 5-hydroxymethylfurfural as side products will be formed.

Several different types of catalyst were used in sugar transformation, for example Sn-modified Beta zeolites have been demonstrated to be promising catalysts in glucose transformations to methyl lactate [6–8, 22–24,26] along with metal modified Y [21] and USY zeolites [9,25], Ni-Hmim-4 [11], Sn loaded in salen ionic liquid [18] and metal modified mesoporous materials, such as MCM-41 [14].

Homogeneous salts as additives have been used together with Sn-Beta to promote methyl lactate formation from sugars [24]. Especially addition of potassium, rubidium and caesium as salts into the reaction mixture has been efficient for Sn-Beta zeolite promoting the methyl

* Corresponding author.
E-mail address: dmurzin@abo.fi (D.Yu. Murzin).

https://doi.org/10.1016/j.micromeso.2023.112483
Received 30 December 2022; Received in revised form 19 January 2023; Accepted 2 February 2023
Available online 3 February 2023

lactate yield [24]. In Ref. [24] 22% yield of methyl lactate was obtained from xylose at 160 °C over Sn-Beta when adding an optimum amount of K_2CO_3 salt into the reaction mixture. Among other products 25% methyl glucosides, 10% furanics, 8% 3-deoxy esters of xylose and 4% 3, 4-dideoxy esters of xylose were reported. The reason for a lower methyl lactate yield when using a high amount of K_2CO_3 salt as an additive was stated to be a slower dehydration rate. The highest yield of methyl lactate from sucrose was 75% at 93% conversion using 0.065 M K_2CO_3 in methanol at 170 °C [18]. In Ref. [25] also $MgCl_2$, $CaCl_2$, and KCl were tested as additives for Sn-Beta catalyst in glucose transformation [26].

Fully heterogeneous tin-modified beta zeolite catalysts have also been intensively studied in glucose transformations with some of the most promising results for formation to methyl lactate summarized in Table 1 [1–4]. For example, Sn loaded on hierarchical Beta zeolite gave 58% methyl lactate yield (Table 1, entry 1) [6]. Different options in general are possible for synthesis of Sn-beta including a hydrothermal procedure using just tetraethyl orthosilicate and tetraethylammonium hydroxide without a T^{III} element like Al^{3+}. However, the presence of Al^{3+} or another T^{III} element is very important in the crystallization of beta zeolites. Moreover, hydrothermal synthesis of siliceous beta zeolites results in hydrophobic materials. Other options include, for example, a fluoride route giving higher hydrophobicity of Sn-Beta and a microporous structure but larger crystals, which impose diffusional limitations. In that case only 47% methyl lactate yield was obtained. Sn-Beta with a hierarchical structure can be synthesized using a method described in Ref. [6]. In fact, apart from in-situ hydrothermal synthesis with a tin precursor when presence of Sn leads to poor crystallization and longer synthesis time, post-synthesis methods can be used when aluminosilicate Sn-Beta undergoes dealumination and then introduction of tin in the framework. In-situ method of Sn-Beta zeolite synthesis gives a possibility of insertion of Sn in the framework of the Beta zeolite and

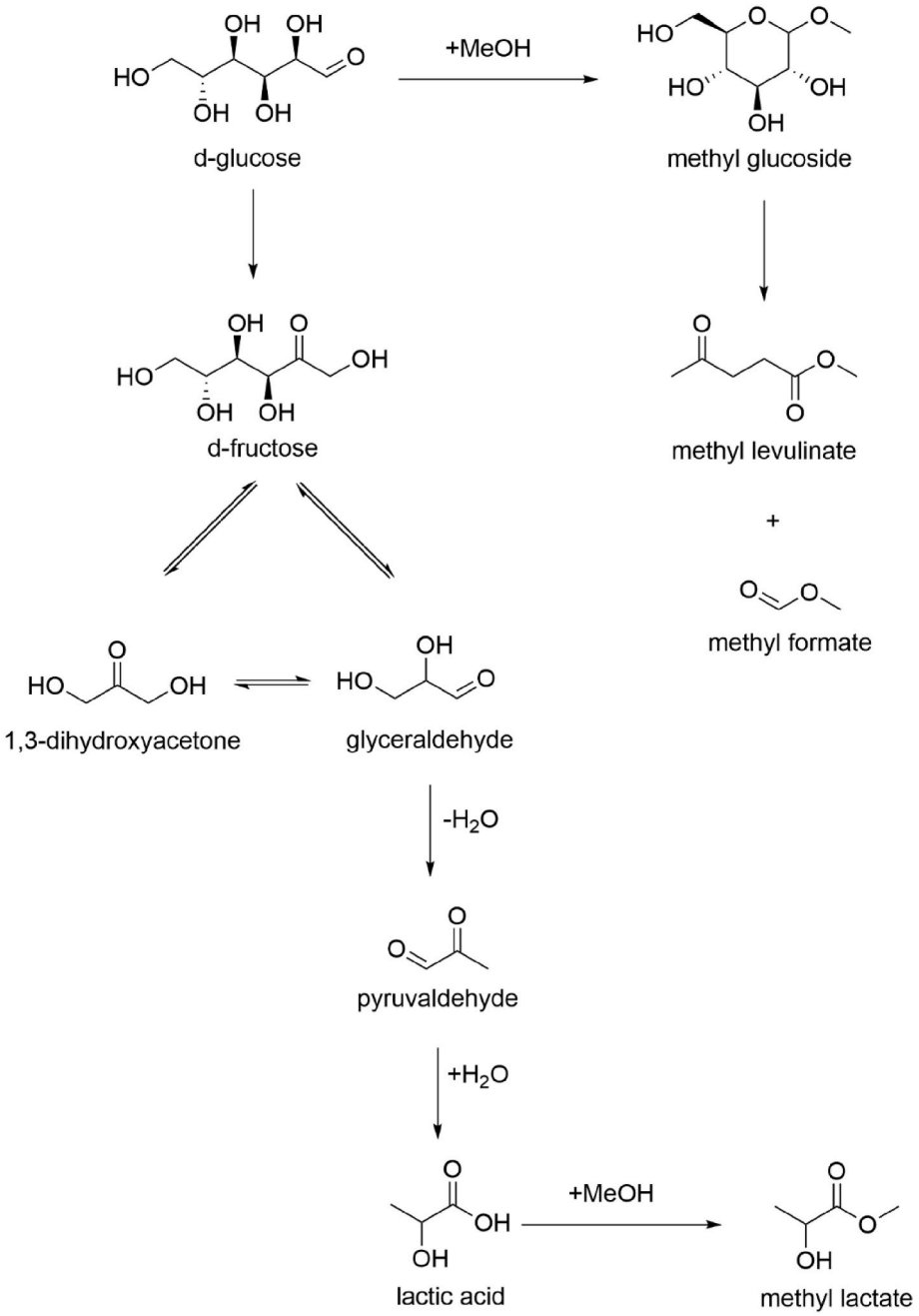

Scheme 1. Glucose transformation to methyl lactate over Sn-modified zeolites.

Table 1
Catalytic results from glucose transformations to methyl lactate.

Entry	Catalyst	Reaction conditions	Methyl lactate yield (%)	Reference
1	Sn-Beta-H-0.3[a]	Glu/cat 1.6 wt/wt, 0.14 mol/l, 160 °C, 5 bar N_2	58	6
2	1 wt% Mg-2 wt% Sn-Beta	Glu/cat 1.85 wt/wt, 0.14 mol/l, 160 °C, 4 bar N_2, 5 h	48	26
3	Zn–Sn-Beta (2.2 wt% SnO_2, 1.5 wt % ZnO)	Glu/cat 2 wt/wt, 0.06 mol/l, 220 °C, 20 bar N_2, 6 h	67	7
4	Fe–Sn/Beta (2.2 wt% SnO_2, 1.4 wt % Fe_2O_3)	Glu/cat 2 wt/wt, 0.06 mol/l, 220 °C, 20 bar N_2, 6 h	67	8
5	Ga-ZnO/H-nano-Y	Glu/cat 4.0 wt/wt, 0.15 mol/l, 270 °C, 10 bar N_2, 1 h	63	21
6	K-Sn-Al-USY	Glu/cat 4.8 wt/wt, 0.26 mol/l, 170 °C, 20 bar N_2, 6 h	44.8	25
7	2 wt% Sn 0.6 wt% K-USY	Glu/cat 4.7 wt/wt, 0.266 mol/l, 150 °C, 20 bar N_2, 6 h	70	9
8	Ni-Hmim-4	Glu/cat 2.0 wt/wt, 0.044 mol/l, 180 °C, 12 h	42	11
9	Sn-Salen IL	Glu/cat 6 wt/wt, 0.06 mol/l, 160 °C, 20 bar N_2, 20 h	41	18
10	1.9 wt% Sn- 1.2 wt% In-MCM-41	Glu/cat 1.4 wt/wt, 0.125 mol/l, 160 °C, 20 h	69	14
11	UZAR-S4	Glu/cat 1.4 wt/wt, 0.013 mol/l, 160 °C, 20 h	49.9	27

[a] indicates the concentration of tetraethyl ammonium hydroxide.

enhanced dispersion of Sn metal nanoparticles. Furthermore, with optimized hydrothermal Beta zeolite synthesis parameters, it is possible to influence the Sn metal nanoparticle size distribution.

Magnesium modified Sn supported on dealuminated Beta zeolite gave 48% methyl lactate yield [26] (Table 1, entry 2) and it was concluded that Mg promoted Sn-Beta enhances the retro-aldol step for fructose in the glucose transformations. The magnesium loading was also optimized in Ref. [26] leading to an observation that with a higher Mg loading the yield of methyl lactate decreased. High magnesium loading gave very high basicity for the catalyst. Furthermore, Lewis acid sites concentration increased also with increasing Mg loading. XPS measurements of 1 wt% Mg- 2 wt% Sn/Beta revealed that Sn was located in the framework.

Very high methyl lactate yields were obtained over a bimetallic Fe–Sn/Beta zeolite being 67% at complete glucose conversion at 220 °C [8] and the same methyl lactate yield was also obtained over Zn–Sn/Beta catalyst [7] (Table 1, entry 3, 4). In Ref. [8] the reaction temperature was rather high for glucose transformations, namely the reported optimum reaction temperature maximizing the methyl lactate yield in the temperature range of 180–240 °C was 220 °C. It was stated in Ref. [8] that $Sn4^+$ has a synergistic effect with Zn^{2+}. Furthermore, it was proposed based on XPS measurements that $Zn^{2}+$ ions occupy vacant tetrahedral sites in partially dealuminated Beta zeolite.

Textural properties of the catalyst have been taken into account by using Ga-doped ZnO/H-nanozeolite Y in glucose transformation giving 64% yield of methyl lactate in supercritical methanol [21]. In the latter case a mesopore directing agent was used to facilitate formation of mesoporous and the catalyst was composed of 200 nm agglomerates containing 10 nm particles. When using nanozeolites a large external surface is created, which is beneficial by enhancing mass transfer. Lewis acidity was promoted in these catalysts by modification of ZnO with Ga [21] (Table 1, entry 5). In addition, dealuminated K-Sn-Al-USY zeolite was a rather efficient catalyst giving the highest methyl lactate yield of 44.8% from glucose transformations at 170 °C and the carbon balance of 57 mol% (Table 1, entry 6) [25]. This catalyst exhibited the lowest Brønsted to Lewis acid ratio among the studied materials. The other main products were glycolaldehyde dimethyl acetal and methyl vinyl glycolate with the yields of 7.5% and 11.2%, respectively. Analogously a direct loading of tin on USY [25] improved selectivity in methyl lactate (Table 1, entry 6). A very high methyl lactate yield was also obtained over potassium modified Sn-USY at a rather low temperature, 150 °C (Table 1, entry 7) [9]. Occurrence of side reactions could be suppressed by addition of potassium to the catalyst which then exhibited a rather low acidity confirmed by ammonia TPD. It was also concluded that lower yields of retro-aldol condensation products including methyl vinyl glycolate, glycolaldehyde dimethyl acetal and methyl glycolate were observed when the alkali cation (K^+) interacts with tin sites [9].

Metal-ionic liquid composite catalysts have also been successfully investigated in glucose transformations [11,20]. For example, Ni in ionic liquid Hmim-4 (Hmim denotes 2-methylimidazole) [11] and Sn(salen)/IL complex immobilized with an ionic liquid [20] were used as catalysts (Table 1, entry 8, 9). The former catalyst was composed of γ-NiOOH phase exhibiting surface area of 126 m^2/g_{cat}, pore size of 10 nm and the Lewis to Bronsted acid ratio of 9.2. It was also observed that an optimum temperature of 180 °C gave the highest yield of methyl lactate and this temperature was required for efficient fructose transformation. Sn(salen)/IL catalyst was less efficient for methyl lactate formation giving only 41% yield at 160 °C. Furthermore, the total yield was only ca. 48%, when small amounts of methyl levulinate, pyruvic aldehyde dimethyl acetal, 5-methoxymethylfurfural and methyl glycolate were also formed. This catalyst was composed of a Sn(salenI)/IL complex prepared via a metallization of ionic liquid functionalized salen complex. The ionic liquid used in the preparation was imidazolium-based [OMIm]Br. A relatively high activity of this catalyst originated form the coordination of Sn^{4+}. Furthermore, $[OMIm]^+$ was stated to promote the proton transfer to the OH leaving group in fructose.

A mesoporous, bimetallic Sn–In-MCM-41 was very selective for transforming glucose to methyl lactate with 69% yield [14] (Table 1, entry 10). It was concluded in Ref. [14] that a synergistic effect between the two metals promoted formation of a higher amount of methyl lactate. Furthermore, noteworthy is that when comparing the performance of Sn–In-MCM-41 with those of Sn-MCM-41 and In-MCM-41, it was observed that the two latter ones gave methyl lactate yield of 56% and 37%, respectively [14]. The corresponding total yields were for Sn–In-MCM-41, Sn-MCM-41 and In-MCM-41 80%, 56% and 37%, which was the decreasing order of Brønsted acid sites in these catalysts. This result indicated that the amount of products, both identified and unidentified eluting from GC and sugars analyzed by a commercial analytical kit was decreasing with an increasing catalyst Brønsted acid site concentration.

Delaminated stannosilicate, which was intercalated with nonylamine (UZAR-S4) and exhibited both strong and weak Lewis acid sites confirmed by ammonia TPD as well as also Brønsted acidity according to FTIR with pyridine, gave 37% methyl lactate yield from glucose at 160 °C. The total yield under these conditions was 59% at 99.5% conversion [27] (Table 1, entry 11). This catalyst produced, however, a rather high amount of pyruvaldehyde acetal (PADA), ca. 6%.

The literature is still rather scarce regarding preparation, characterization and testing alkali-modified zeolites in glucose transformation to methyl lactates. In particular, no quantitative analysis of alkali content and dependence of selectivity on Lewis/Brønsted acidity is available, which can be critical for achieving high selectivity to methyl lactate.

The concentration of Brønsted acid sites might be too high in such materials, thus there is a need to suppress them. Moreover, weak basic sites were reported to be beneficial for methyl lactate formation as

mentioned above. Subsequently the aim in this work was to investigate the effect of addition of different amounts of K_2CO_3 in the reaction mixture together with Sn–Al-Beta catalyst in glucose transformations to methyl lactate. Such approach was anticipated to be a viable alternative to Sn-Beta catalysts prepared without Al, which were reported to be selective in glucose to methyl lactate transformations.

Furthermore, different alkali metal modified Sn–Al-Beta zeolite catalysts were synthesized, characterized and tested in this reaction. The following alkali metals were tested as modifiers for Sn-Beta: K, Ca, Mg, Sr and Ba. While limited data are available for K, Ca and Mg, according to our knowledge Sr and Ba have not been investigated previously.

2. Experimental

2.1. Catalyst preparation

Synthesis of Sn–Al-Beta was carried out by first preparing a solution (A) containing 179.2 g tetraethyl ammonium hydroxide solution, 118.8 g distilled water, 2.88 g KCl, 1.06 g NaCl, 3.56 g $SnCl_2{\cdot}2H_2O$ and 60 g of fumed silica. The other solution (B) contained 0.66 g NaOH, 3.58 g $NaAlO_2$ and 20 ml distilled water. The two solutions were mixed and stirred for 20 min, forming a gel. The gel was thereafter crystallized under rotation to a solid material at 150 °C for 120 h. After crystallization the solid material was washed thoroughly with distilled water, dried and finally calcined at 530 °C for 6 h in order to remove the organic template.

The prepared Sn–Al-Beta zeolite was further modified through incipient wetness impregnation using aqueous solutions of K_2CO_3, KNO_3, $Ca(NO_3)_2$, $Mg(NO_3)_2$, $Sr(NO_3)_2$ having a concentration of 0.7 mol/l and $Ba(NO_3)_2$ with a 0.3 mol/l concentration due to limited solubility. After the impregnations the catalysts were dried and calcined at 530 °C for 6 h to decompose the metal precursor. The prepared catalysts are denoted as K_2CO_3–Sn–Al-Beta, KNO_3–Sn–Al-Beta, Ca–Sn–Al-Beta, Mg–Sn–Al-Beta, Sr–Sn–Al-Beta and Ba–Sn–Al-Beta.

2.2. Glucose conversion experiments

The glucose conversion experiments were carried out by loading the reactor vessel with 0.41 g of the catalyst (<63 μm), 0.9 g glucose (>98%, Fluka) and 100 ml methanol (>99.9%, Sigma-Aldrich). Experiments with higher glucose concentrations were not pursued because of a limited solubility of glucose in methanol [29]. After filling the reactor with the reactants and the catalyst, it was flushed with argon. Thereafter, heating to 180 °C was started with a 3 °C/min heating rate. When the reactor temperature reached 180 °C and the total pressure was adjusted to 30 bar, the sampling (t = 0 min) and stirring (720 rpm) were started. Due to the small catalyst particle size and high stirring speed internal and external mass transfer limitations were suppressed. The samples were withdrawn from the reactor through a 7 μm sinter to avoid removal of catalyst particles, moreover, prior to analysis the liquid samples were further filtered through a 0.43 μm syringe filter. Prior to taking a sample, 1 ml of the waste sample was withdrawn from the reactor to have representative sampling. The sample volume was 1.5 ml. The samples were initially analyzed by HPLC, and by GC after achieving practically full sugar conversions.

The influence of added K_2CO_3 to the reaction mixture was investigated in the concentration range 0–1.25 mmol/l using the parent Sn–Al-Beta as the catalyst.

2.3. Product analysis

The composition of the reaction mixture was analyzed by high performance liquid chromatography (HPLC). The HPLC (Hewlett Packard 1100 series) was equipped with a refractive index detector (RI), while the column used for separation of the compounds was an Animex HPX-87H applying 5 mM sulphuric acid as the eluent. The temperature of the column was 45 °C and the flow of H_2SO_4 was 0.6 ml/min. Response factors as well as retention times for several different compounds were determined prior to catalytic experiments and used for calculations of the concentrations. After achieving in practice full conversion of glucose the sample was further analyzed by gas chromatography to quantify methyl lactate and methyl levulinate as well as furfural and methyl formate. The GC used was an HP 6890 Series GC System with an HP-5, 5% phenyl methyl siloxane 30.0 m × 320 μm x 0.50 μm column. The eluting components were detected by a flame ionisation detector (FID). The temperature program used in the analysis was as follows: 2 min at 40 °C, heating with 10 °C/min to 250 °C and holding for 3 min, the gas flow through the column was set to 3.8 ml/min.

2.4. Definitions

The conversion of glucose (X) was calculated by:

$$X = \frac{n_{glu,0} - n_{glu,t}}{n_{glu,0}} * 100\% \quad (1)$$

where $n_{glu,0}$ is the initial glucose molar concentration and $n_{glu,t}$ is the glucose molar concentration at time t.

The liquid phase mass balance of compounds (MB) was calculated by:

$$MB = \frac{MB_t}{MB_0} * 100\% \quad (4)$$

where MB_t is the sum of liquid-phase reactants and products at time t, and MB_0 is the sum of liquid-phase reactants and products at the beginning of the reaction (time 0). The compounds that are not included in eq. (4) are gas-phase products, and heavy compounds adsorbed on the catalyst (carbon deposits/coke).

The carbon balance (CB) was calculated by:

$$CB = \frac{\sum n_{i,t} \bullet CN_i}{n_{glu,0} \bullet CN_{glu}} * 100\% \quad (5)$$

where $n_{i,t}$ is molar concentration of i compound considered in eq. (4) at time t, and CN is the carbon number.

Yields of products ($Y_{i,t}$) were calculated by relating the molar concentration of a particular product $n_{i,t}$ to the initial concentration of glucose $n_{glu,0}$ considering also the reaction stoichiometry

$$Y_{i,t} = \frac{n_{i,t}}{s\, n_{glu,0}} * 100\% \quad (6)$$

Where s is the stoichiometric coefficient (e.g. 2 for methyl lactate and 1 for methyl levulinate).

The initial reaction rates (r) are calculated in the time range of 15–45 min as follows:

$$r = \frac{\Delta n}{\Delta t . m_{cat}} \quad (7)$$

2.5. Catalyst characterization

The prepared metal modified catalysts were characterized with different techniques. The concentration of Brønsted and Lewis acid sites was measured using FTIR and pyridine as the probe molecule. Both scanning and transmission electron microscopy was used to elucidate morphology and the textural properties. The specific surface area and the pore size distributions were determined by nitrogen physisorption. The phase purity of the catalysts was confirmed by XRD. More details are provided below.

A FTIR (ATI Mattson Infinity Series) was used for determining the strength and concentrations of both Brønsted and Lewis acid sites. The metal modified Beta zeolites were pressed into thin wafers and placed into the FTIR cell, which was outgassed and heated to 450 °C for 1 h.

Thereafter, the cell was cooled to 100 °C and the background spectrum was recorded. Pyridine (>99%, Acros Organics) was adsorbed on the catalytic acid sites during 30 min followed by desorption at 250 °C, 350 °C and 450 °C under vacuum for 1 h at each temperature. Spectral bands at 1545 cm^{-1} and at 1450 cm^{-1} were used to identify Brønsted (BAS) and Lewis (LAS) acid sites. The concentrations of acid sites were calculated using the extinction coefficients reported by Emeis [30].

The ^{29}Si and ^{27}Al MAS NMR spectra was recorded on a Bruker AVANCE-III spectrometer operating at 79.50 MHz (^{29}Si) and 104.26 MHz (^{27}Al) equipped with a CP-MAS 4 mm solid state probe. The ^{27}Al spectra was recorded using a 5.00 μs pulse and a recycle delay of 0.05 s at 14 kHz spinning speed. The ^{29}Si spectra was recorded using a 3.84 μs pulse and a recycle delay of 100 s at 14 kHz spinning speed.

The crystal morphology, shape and size of the catalysts were studied with Scanning Electron Microscopy (SEM) using a (Leo Gemini 1530) microscope. The presence of metal nanoparticles and porosity of the catalysts were investigated by Transmission Electron Microscopy (TEM) using a (JEOL JEM-1400 Plus) microscopy equipped with a bottom mounted (OSIS Quemesa) digital camera.

The specific surface area, pore size and the pore volume of the catalysts were measured with Micrometrics MicroActive 3Flex3500. Prior to the surface area measurements, the catalyst samples were outgassed at 250 °C for 4 h. The specific surface was calculated with the Dubinin-Radushkevich method and the pore size and volume with the Horvath-Kawazoe method.

The elemental composition of the catalysts was determined by Spectro Xepos EDXRF. A simple leaching test was carried out at room temperature by keeping the catalysts in methanol for 24 h (analytical grade). The elemental composition of the leached catalyst was determined by EDXRF and the leachate by ICP-MS.

The X-ray diffraction (XRD) characterization was performed using a (PANalytical Empyrean) diffractometer. The results were obtained with a 2θ scan range from 5° to 90°.

3. Results and discussion

3.1. Catalyst characterization results

The XRD pattern for the parent Sn–Al-Beta and the standard structure for Beta polymorph A displayed in Fig. 1 shows that the prepared Sn–Al-Beta zeolite has a XRD pattern that can be attributed to the presence of Beta polymorph A, confirming that the prepared material exhibits in fact the Beta zeolite structure. Comparison of the XRD patterns for Sn–Al-Beta and the polymorph A also points out on the presence of the polymorph B in the synthesized material.

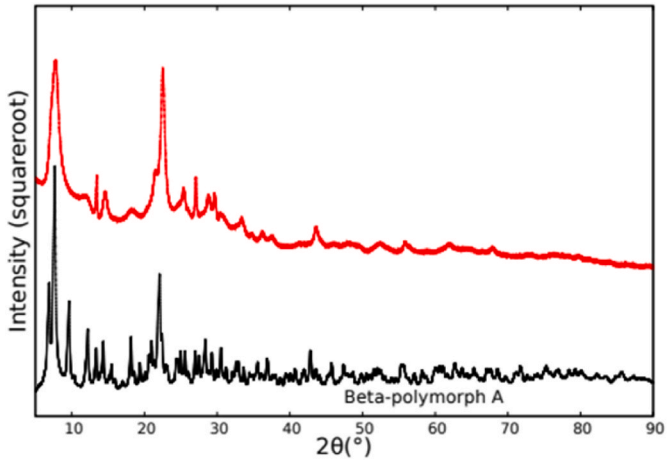

Fig. 1. XRD results for the Sn–Al-Beta catalyst with a standard structure for Beta polymorph A [32].

Analysis of SEM image of the parent Sn–Al-Beta catalyst gives the average crystal size of 604 ± 35 nm (Fig. 2).

TEM images of the Sn–Al-Beta, displayed in Fig. 3, do not show presence of nano-sized tin particles, illustrating that tin is well dispersed.

The specific surface area, the pore size and the volume were measured with nitrogen physisorption with the results gathered in Table 2. Modification with different alkali and alkaline earth metals showed only minor changes (namely a slight decrease) in the surface area, while the pore sizes (Table 2, Fig. 4) of ca. 0.63–0.64 nm, their distribution (Fig. 4) and pore volume for all catalysts, 0.17 ml/g were essentially the same.

The concentrations of Brønsted (BAS) and Lewis acidity (LAS) of the parent Sn–Al-Beta zeolite as well as for catalysts modified by incipient wetness impregnation are presented in Table 3.

From Table 4 it can be clearly observed that the concentrations of Brønsted acidity decreased when the Sn–Al-Beta zeolite is modified with different alkali and alkaline earth metals. An analogous trend with alkali metal modified Sn-USY with decreased Brønsted acidity was determined by DRIFT spectroscopy in Ref. [25], while Lewis acidity remains constant. Furthermore, Lewis acidity is increased when the Sn–Al-Beta is modified with calcium or magnesium, while a smaller increase is observed for the strontium modified catalyst and in practice no changes in Lewis acidity were observed for the potassium modified Sn–Al-Beta. Barium modification did not change the acid site distribution significantly.

The effect of adding different concentrations of K_2CO_3 to the reaction mixture on the acidity of regenerated Sn–Al-Beta is presented in Table 4. Prior to measurements the spent catalyst was recovered through filtration and regenerated at 400 °C in air to remove possible carbon deposits. The catalyst named Sn–Al-Beta REG is the regenerated Sn–Al-Beta catalyst without any K_2CO_3 addition.

A clear decrease in Brønsted acidity can be seen when adding K_2CO_3. An interesting maximum in Lewis acidity is observed at K_2CO_3 concentrations of 0.5–1.0 mmol/l which corresponds to the same range as maximizing the methyl lactate yield. It is difficult to make any comparison of catalyst acidity values when adding K_2CO_3 into the reaction mixture with the literature data, because in Ref. [24] acidity of the catalysts in the presence of K_2CO_3 was not determined. A maximum in Lewis acidity upon exposure to potassium carbonate with different concentrations could not be easily anticipated, requiring an additional investigation by e.g. NMR to reveal speciation of Lewis sites after such treatment, similarly to the NMR results presented below for different alkali- and alkaline earth metals. Moreover, apparently not only the nature of the alkali or alkali-earth metals influences the

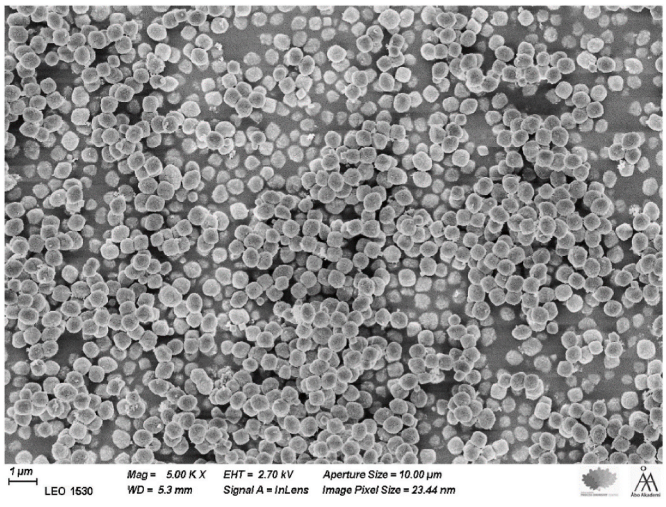

Fig. 2. SEM image for Sn–Al-Beta catalyst.

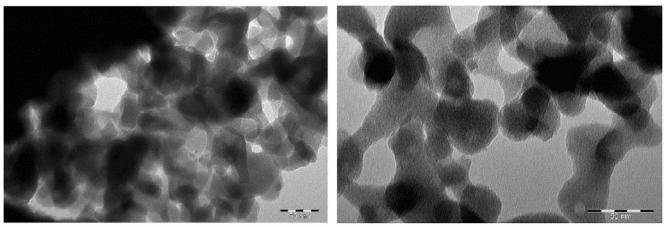

Fig. 3. TEM images of Sn–Al-Beta catalyst.

Table 2
Specific surface area, pore size and volume for the parent and modified with K_2CO_3, KNO_3, $Ca(NO_3)_2$, $Mg(NO_3)_2$ and $Sr(NO_3)_2$ Sn–Al-Beta catalysts.

Catalyst	Specific surface area (m^2/g)	Pore size (nm)
Sn–Al-Beta	491	0.64
K_2CO_3–Sn–Al-Beta	466	0.63
KNO_3–Sn–Al-Beta	482	0.63
Ca–Sn–Al-Beta	472	0.64
Mg–Sn–Al-Beta	486	0.64
Sr–Sn–Al-Beta	472	0.64

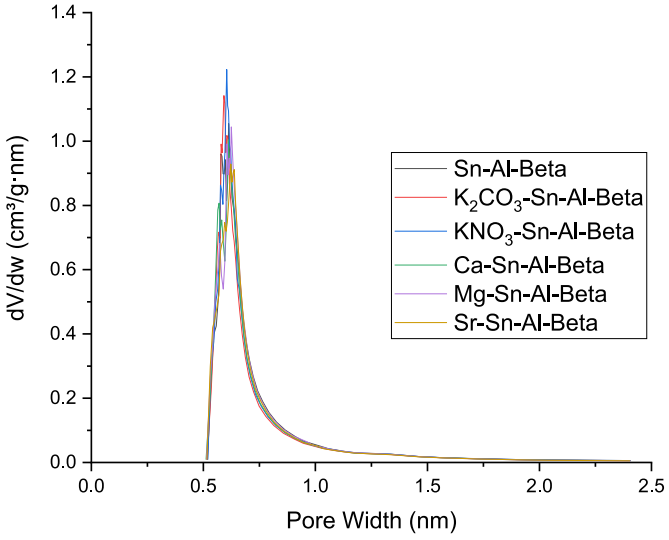

Fig. 4. Pore size distribution for parent and alkali modified Beta zeolites.

Table 3
Concentrations of Brønsted and Lewis acid sites at different pyridine desorption temperatures for the modified Sn–Al-Beta catalysts[a].

Catalyst	Brønsted acid sites (μmol/g)			Lewis acid sites (μmol/g)		
	250 °C	350 °C	450 °C	250 °C	350 °C	450 °C
Sn–Al-Beta	238	217	140	114	27	9
K_2CO_3–Sn–Al-Beta	110	88	48	105	11	3
KNO_3–Sn–Al-Beta	138	121	77	119	20	6
Ca–Sn–Al-Beta	125	112	90	170	44	19
Mg–Sn–Al-Beta	163	125	110	174	70	38
Sr–Sn–Al-Beta	126	120	40	159	39	4
Ba–Sn–Al-Beta	173	166	109	122	30	5

[a] Details of the characterization method are provided in Section 2.5. Catalyst characterization.

physico-chemical properties of zeolites, but also the concentration of the alkali metal cations.

The concentrations of Sn, Al, K, Mg, Ca, and Sr of fresh and leached catalysts as well as concentrations of the leachate are listed in Table S1.

For each material in the second column the concentrations of the elements are given, while the corresponding values in the leached catalyst and in the liquid (the leachate) are given in the third and fourth columns respectively. Within the precision of the analysis it can be stated that no major leaching of the metals occurred during the leaching test. It should be noted that the targeted value of tin loading was 2.9% in line with the literature reports illustrating that the values of tin loading determined by SEM-EDX are rather close to the targeted ones.

The discrepancy for the fresh and leached KNO_3–Sn–Al-Beta with the concentrations of K are 0.98 wt% and 1.0 wt% respectively can be attributed to precision of the analysis.

Table 4
Concentrations of Brønsted and Lewis acid sites at different pyridine desorption temperatures for Sn–Al-Beta with different concentration of added K_2CO_3 to the reaction mixture.

Catalyst	Brønsted acid sites (μmol/g)			Lewis acid sites (μmol/g)		
	250 °C	350 °C	450 °C	250 °C	350 °C	450 °C
Sn–Al-Beta	238	217	140	114	27	9
Sn–Al-Beta REG	191	171	42	94	28	15
0.065 mM	214	197	101	102	25	18
0.17 mM	195	184	51	100	23	15
0.5 mM	108	92	31	149	22	6
0.625 mM	117	102	51	146	22	6
0.75 mM	89	76	22	187	22	3
1.0 mM	54	35	6	135	11	2
1.25 mM	45	25	4	119	8	1

The results from the solid state NMR show (Fig. 5a) that the peak area at ca. 0 ppm corresponding to hexacoordinated aluminium which are extra-framework species decreased as follows: Sn–Al-Beta > Na–Al-Beta > Sr–Sn–Al-Beta > K_2CO_3–Sn–Al-Beta > Ba–Sn–Al-Beta.

Note that the sodium modified sample was used only as a reference in NMR analysis. Furthermore, the intensity of the peak at 54 ppm related to tetrahedral aluminium species in the framework responsible for Brønsted acidity in zeolites [33] is nearly the same for all catalysts. It is also known that hexacoordinated aluminium species exhibit Lewis acidity [34], which are extra-framework species [31]. When correlating these to the FTIR pyridine results (Table 4), it can be seen that when the ratio of BAS to LAS determined by pyridine adsorption desorption was plotted as a function of the ratio between the peak areas at 54 ppm–0 ppm corresponding to Brønsted and Lewis acid sites, a linear correlation for this ratio was observed both for FTIR pyridine adsorption desorption and for ^{27}Al NMR measurements as follows: Sr–Sn–Al-Beta < K_2CO_3–Sn–Al-Beta < Ba–Sn–Al-Beta, while the parent Sn–Al-Beta exhibited the highest BAS/LAS ratio only with pyridine adsorption-desorption method (Fig. 5b).

The results from ^{29}Si NMR suggest that the intensity of the peak close to −113 ppm (Fig. 5b) representing the framework Si[OSi]$_4$ (Q^4) sites [35] is the same, while the intensity of the peak close to −103 ppm denoting framework Si(OSi)$_3$(OH) species (SiOH groups, Q3) [36] is the highest for Ba- and Sn–Al-Beta zeolites.

3.2. Glucose transformations results

3.2.1. Glucose transformation over alkali modified Sn–Al-Beta catalysts

Glucose transformation was investigated with alkali metal modified Sn–Al-Beta catalysts (Fig. 6). The results showed that glucose conversion after 15 min of the reaction time was above 98% for KNO_3-modified Sn–Al-Beta zeolite, while more than 97% glucose conversion was observed at 15 min for Ca-, Mg-, Sr– Sn–Al-Beta catalysts. The lowest conversion of glucose was 96% for Ba-modified Al-Beta zeolite at 15 min. After 1440 min complete glucose conversion was obtained with all catalysts. The carbon balance was the lowest for Mg–Sn–Al-Beta followed by Ca–Sn–Al-Beta, while the two highest carbon balances were obtained with Ba- and KNO_3 modified Sn–Al-Beta catalysts (Table 5). Note that the carbon balance is calculated based on the yields in Table 5, thus for lower balance closures other products than the ones listed in

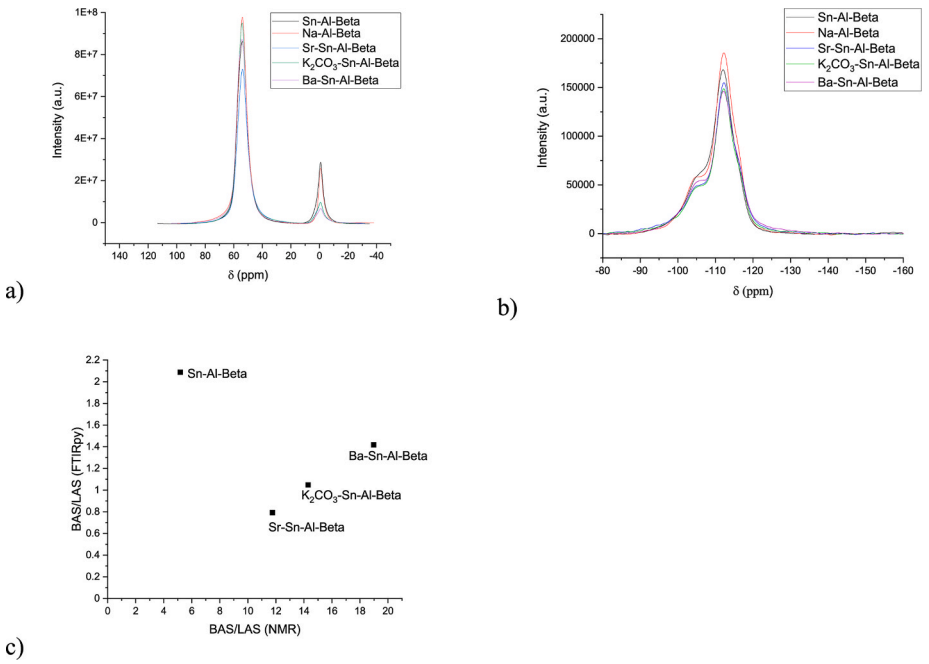

Fig. 5. NMR spectra of a) ^{27}Al, b) ^{29}Si and c) the ratio BAS/LAS determined by pyridine adsorption desorption plotted as a function of the ratio of the peak area at 54 ppm–0 ppm corresponding to Brønsted and Lewis acid sites.

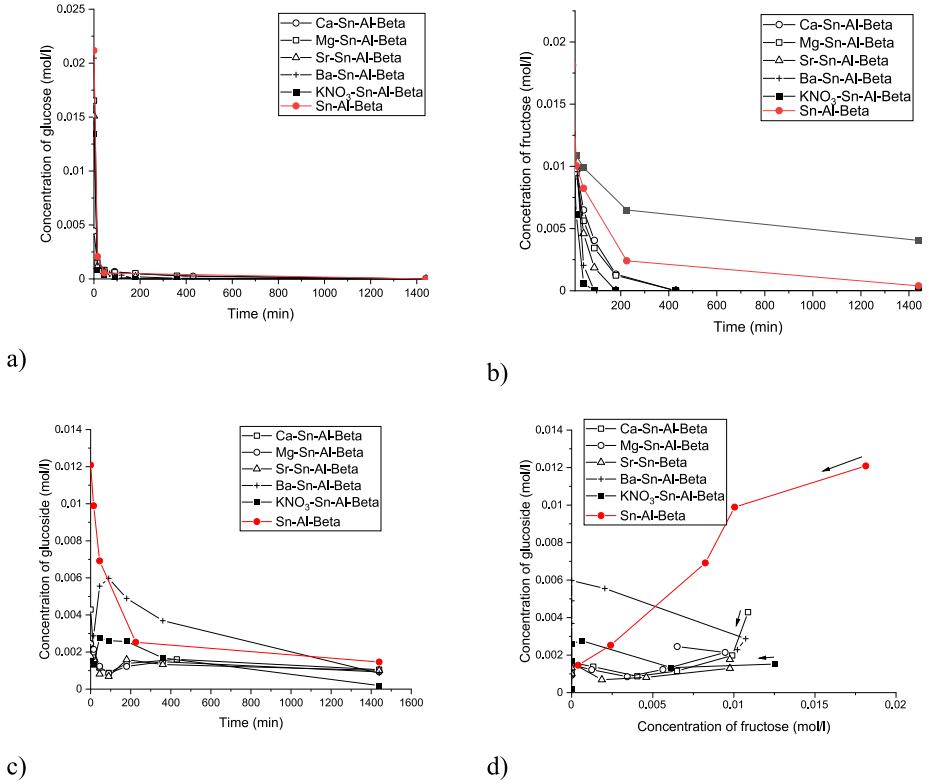

Fig. 6. Concentration of a) glucose, b) fructose, c) methyl glucosides as a function of time and d) concentration of methyl glucoside as a function of concentration of fructose over alkali metal modified Sn–Al-Beta catalysts. The arrow indicates an increase of the reaction time. Reaction conditions: $c_{0,\ glu} = 5$ mmol, $V_L = 100$ ml, $m_{cat} = 0.41$ g, solvent methanol, 180 °C under 30 bar total pressure under Ar after 1440 min.

Table 5 are most likely formed.

No optimization of the reaction time has been attempted in the current work and the data in Table 5 correspond to a rather long reaction time relevant in the context of methyl lactate yields when essentially all sugars (glucose, fructose and methyl glucosides) have been transformed. Even if almost complete conversion could be achieved within ca. 15 min, the final samples were intentionally taken at 1440 min showing in most cases only traces of the sugars.

According to stoichiometry methyl formate is formed in equimolar amounts with methyl levulinate. The apparent discrepancy in the yields

Table 5
The yields of products determined by GC analysis as well as the yield of methyl glucosides determined by HPLC over different catalysts at 180 °C after 1440 min.

Catalyst	Methyl levulinate (%)	Methyl lactate (%)	Furfural (%)	Methyl formate (%)	Methyl glucosides (%)	Carbon balance (%)	Total yield of products (%)
Sn–Al-Beta	31.4	19.5	2.5	19.5	0	46.0	72.9
K_2CO_3–Sn–Al-Beta	1.5	53.3	4.5	0	1.0	57.2	60.3
KNO_3–Sn–Al-Beta	17.0	41.8	1.9	4.8	0.4	63.4	65.9
Ca–Sn–Al-Beta	1.9	39.8	3.4	1.2	2.1	44.5	48.4
Mg–Sn–Al-Beta	1.9	37.5	3.9	1.9	1.8	42.9	46.9
Sr–Sn–Al-Beta	5.3	53.2	5.3	2.7	2.0	63.6	68.5
Ba–Sn–Al-Beta	22.8	30.6	2.9	7.6	1.7	61.0	65.6

of these two compounds can be explained by a much lower boiling point of methyl formate (only 32 °C), which can result in losses prior to analysis.

In comparison with literature [13] analogous results with the lowest carbon balance determined for Mg and Ca modified Sn-Al-USY were obtained in glucose transformation at 170 °C, while Na and K modified catalysts gave a higher carbon balance. It should also be pointed out here that the kinetic diameter of glucose is 0.86 nm [37] indicating that glucose is reacting mainly on the outer surface of the catalyst, because the pore size of Beta- zeolite catalysts is 0.64–0.65 nm (Table 2).

Fig. 6 shows the concentration of reaction intermediates in the formation of methyl lactate. In fact, GC analysis of fructose and methyl glucosides in methanol is highly challenging as these compounds with high boiling points require derivatization. This is also the reason why GC analysis was performed at prolonged reaction times at high conversion of sugars. As these compounds are eventually transformed into methyl lactate, it is instructive to follow their transformations by HPLC.

The main initial products observed in HPLC chromatograms were fructose (Fig. 6b) and α− and β-methyl glucosides (Fig. 6c). The former one is formed by isomerization of glucose in methanol and being catalysed according to Ref. [38] by extra-framework Sn species. Methyl glucosides are formed by glucosidation of glucose and methanol over Brønsted acid sites [39]. The presence of methyl glucosides was confirmed by NMR in Ref. [40] and the peak in the current work with the same retention time as was interpreted as methyl glucoside in Ref. [40]. Furthermore, no mannose was detected in the reaction mixture, even if in Ref. [39] it was also confirmed that mannose is formed from glucose over framework Sn sites.

The highest concentration of fructose after 90 min was obtained for Ca-modified Sn–Al-Beta zeolite followed by Mg, and Sr (Fig. 6b), while K- and Ba-modified Sn–Al-Beta catalysts transformed rapidly fructose. KNO_3- modified Sn–Al-Beta and Ba–Sn–Al-Beta exhibited high Brønsted acid sites concentrations while Lewis acidity was rather low. No methyl fructosides were visible in the reaction mixture in the current case opposite to the results in Ref. [39], in which acidity was investigated by ammonia TPD preventing a direct comparison of acidity values with the current work. However, qualitatively it can be stated that in Ref. [39] most of the acid sites were of weak and medium strength. In the current work the highest concentration of methyl glucosides was determined over unmodified Sn–Al-Beta catalyst with a high concentration of Brønsted acid sites (Fig. 6c). Over alkali metal modified Sn–Al-Beta catalysts Ba–Sn–Al-Beta zeolite gave a high glucoside concentration at 90 min, being 0.004 M. This catalyst exhibited the highest concentration of Brønsted acid sites among alkali modified Sn–Al-Beta catalysts. Glucosidation is a reversible reaction and typically glucoside concentration decreased after increasing reaction time, especially for K–Sn-Beta and for Sn-Beta in Ref. [35]. Furthermore, for Sr-, Mg- and Ca- modified Sn–Al-Beta methyl glucoside concentration remained quite unchanged after 180 min. When plotting the concentration of the primary product glucoside as a function of another primary product fructose (Fig. 6d), it can be seen that both of them are present initially in the reaction mixture and then reacting further.

The promoting effect of different alkali and alkaline earth metals on the methyl lactate yield can be clearly observed (Table 5). The best performing promoters were K_2CO_3 and $Sr(NO_3)_2$ showing a high methyl lactate yield exceeding 50%, while KNO_3, $Ca(NO_3)_2$ and $Mg(NO_3)_2$ displayed a yield of approximately 40%. Interestingly, KNO_3 showed a fairly high methyl levulinate yield compared to other catalysts. The influence of barium was not as pronounced as of other tested promoters giving only a small improvement compared to the parent Sn–Al-Beta catalyst. Utilization of both K_2CO_3 and $Sr(NO_3)_2$ as promoters resulted in a slightly higher methyl lactate yield compared to addition of K_2CO_3 to the reaction mixture shown in Section 3.2.2. When plotting methyl lactate yield as a function of either BAS or LAS it can be seen that with increasing Brønsted acid site concentration lower methyl lactate yields were obtained (Fig. 7), which is in accordance with [25]. The correlation with the Lewis acid site concentration and the methyl lactate yield is less apparent, but can point out on a potential optimum of LAS giving the highest methyl lactate yield.

It should be also noted that the catalytic behaviour of Sn–Al-Beta zeolites modified with alkali and alkali-earth metals studied in the current work was mainly ascribed to changes in acidity/basicity, while in general other possible explanations can be invoked, such as the ionic radii of the metals or their role as co-catalysts. The former values differ for barium and strontium ions being 0.135 and 0.113nm respectively. Moreover, barium salts have been reported as catalysts for direct aldol condensation of β, γ- unsaturated ester donors [41], while strontium oxide supported on alumina with properties of bases exhibited efficient catalytic performance in retro aldol condensation of diacetone alcohol [42]. Apparently an in-depth theoretical study revealing the origin of the difference in metal salts performance, in particular their role as co-catalysts, is warranted.

The highest yields of the undesired methyl levulinate were observed for Sn–Al-Beta, followed by Ba–Sn–Al-Beta and KNO_3–Sn–Al-Beta which also exhibited high concentrations of strong Brønsted acid sites, i.e. 140, 109, and 77 mmol/g_{cat} (Table 3). It should, however, be noted that despite a low concentration of strong acid sites, Ca–Sn–Al-Beta did not catalyse methyl levulinate formation. When comparing the yields of methyl levulinate with the concentrations of methyl formate, it can be stated that high volatility of methyl formate caused its evaporation, as otherwise equimolar amounts of these esters should be formed. In addition, high yields of furfural were determined for Ba–Sn–Al-Beta and KNO_3–Sn–Al-Beta, which both exhibited high amounts of strong Brønsted acid sites. An exception was again Ca–Sn–Al-Beta giving only a minor yield of furfural in comparison to expectations judging from its acidity. From the mechanistic viewpoint furfural is most likely formed from dehydration of pentoses, however, no pentoses have been detected with HPLC analysis employed in the current work. These observations including a potential route to furfural apparently require a separate investigation.

The effect of the alkali metal precursor and the preparation method were also tested for K–Sn–Al-Beta (Fig. 8). The results revealed that nearly the same glucose conversions were obtained with K_2CO_3 and KNO_3 modified Sn–Al-Beta catalysts, when conversion after 15 min was 98.1% for the former one and 98.4% for the latter one. As can been seen from Table 3, the Brønsted acid concentration of the former one was

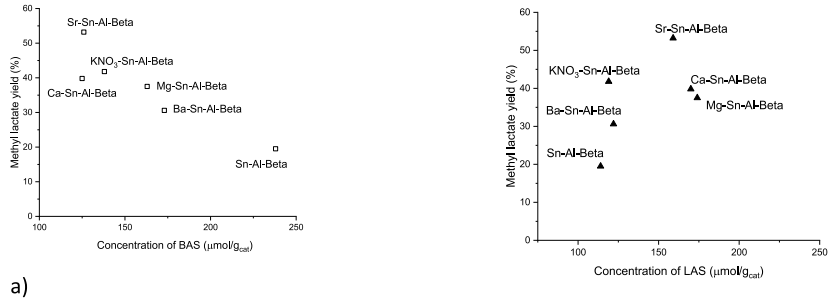

Fig. 7. The yield of methyl lactate after 1440 min in glucose transformation over different alkali metal modified catalysts as a function of the concentration of a) Brønsted or b) Lewis acid sites. Reaction conditions: $c_{0,\ glu} = 5$ mmol, $V_L = 100$ ml, $m_{cat} = 0.41$ g, solvent methanol, 180 °C under 30 bar total pressure under Ar after 1440 min.

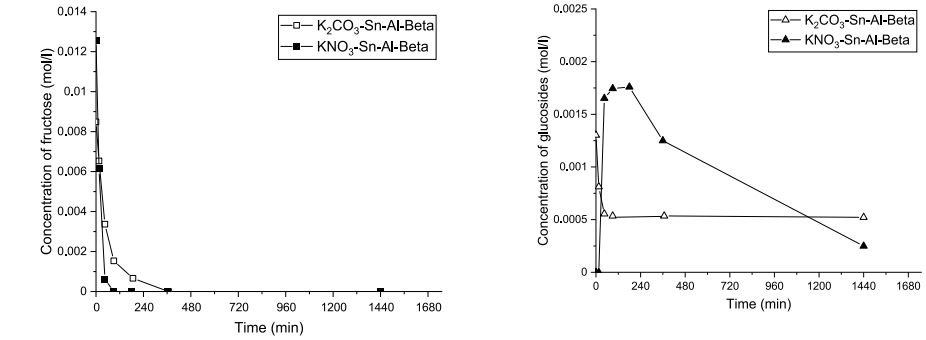

Fig. 8. Comparison of the concentration of a) fructose and b) methyl glucosides as a function of time over KNO_3- and K_2CO_3 modified Sn–Al-Beta catalyst in glucose transformation.

19% lower than for KNO_3 modified Sn–Al-Beta catalyst. As can be seen from Fig. 8b fructose transformation over K_2CO_3 modified catalyst was slower that over KNO_3 modified counterpart. Fructose transformations between 15 and 45 min over K_2CO_3-modified Sn–Al-Beta were only 17% compared to KNO_3–Sn–Al-Beta catalyst, which can be explained by a higher concentration of Brønsted acid sites in the latter catalyst. Analogously a higher amount of Brønsted acid sites in KNO_3–Sn–Al-Beta facilitated fast glucosidation as well as its reverse reaction, while K_2CO_3–Sn–Al-Beta with 48 μmol/g_{cat} of strong acid sites was not able to catalyse ether hydrolysis (Fig. 8).

In GC analysis after complete conversion of the sugars four different products were identified, namely methyl lactate, methyl levulinate, furfural and methyl formate (Table 5). According to the proposed reaction network [25] fructose reacts to 5-hydroxymethylfurfural (HMF) and further to methyl levulinate via ring opening, dehydration and esterification over Brønsted acid sites. Another route is Lewis acid catalysed fructose formation, in which glucose 1,2-enediol is formed in the first step and fructose is formed via keto-enol tautomerization [28]. Thereafter fructose decomposition gives glyceraldehyde and dihydroxyacetone which further react to pyruvaldehyde. This intermediate can react with methanol forming a hemiacetal, which can be further converted to methyl lactate [28].

In the current work neither intermediate trioses nor HMF were observed apparently due to their reactivity under reaction conditions. Besides reacting to methyl levulinate and methyl formate HMF alternatively results in humins, which cannot be analyzed with HPLC or GC. The yields of the four identified products by GC analysis and one via HPLC at 1440 min reaction time are reported in Table 5. Furthermore, the total yield is also reported being in the range of 46.8–80.6% indicating that presence of humins and volatile components is diminishing the liquid phase mass balance closure. Moreover, even the boiling point of methyl formate present in the liquid phase is rather low being 32 °C. Formation of HMF, methyl levulinate and methyl formate is catalysed by Brønsted acid sites, while for methyl lactate generation mainly Lewis acid sites are required. As can be seen from Table 5, the lowest yields of remaining, undesired methyl glucosides were observed over Sn–Al-Beta and KNO_3–Sn–Al-Beta (Fig. 8b).

When comparing the current results with those found in literature (Table 7) a rather high yield of methyl lactate was obtained over nanosized dealuminated Sn-Beta-9 h, in which Sn was confirmed to be in the framework by XPS measurements. The crystallization time was also optimized being 9 h for the best catalyst. In addition, it was stated that mesoporosity enhanced methyl lactate formation. This catalyst did not contain any Brønsted acid sites. A slightly higher yield of methyl lactate was obtained over a hierarchical Sn-Beta-H4, which exhibited Lewis acid site concentration of 50 μmol/g [22], while in the current case the Lewis acid site concentration at the same evacuation temperature for pyridine (250 °C) in FTIR was 159 μmol/g for Sr–Sn–Al-Beta. Furthermore, XPS analyses revealed that Sn-Beta-H4 exhibited Sn partially in

Table 7
Comparison of the obtained methyl lactate yields form glucose over different catalysts.

Catalyst	Conditions	Methyl lactate yield (%)	Reference
Sn-Beta-9 h	0.5 MPa N_2, 160 °C, 10 h	47	[23]
Sn-Beta-H4[a]	0.5 MPa, 160 °C, 6 h	52	[22]
Sr–Sn–Al-Beta	0.3 MPa, 180 °C, 1440 min	53	Current work
Sn–In-MCM-41	160 °C, 20 h	69	[14]

[a] Notation H4 indicates the amount of a mesoporous directing agent.

the framework as well as in a hydrolyzed state. While overall, it can be concluded that the current result with Sr–Sn–Al-Beta is rather promising, however, mesoporous Sn–In-MCM-41 gave even a higher methyl lactate yield. This catalyst contained In and Sn in the oxidation states 3+ and 4+ on the surface of the MCM-41 and both Brønsted and Lewis acidity.

For the reuse of Sr–Sn–Al-Beta catalyst, it was regenerated at 400 °C in air prior to the subsequent test. The results showed that the methyl lactate yield decreased from 47% in the first experiment with the fresh catalyst to 21% and 10% in the following ones showing that it was not possible to recover catalytic performance. Analogously it was found in Ref. [25] that catalytic activity of Sn-Al-USY was not retained and lower carbon balance was obtained, when the catalyst was calcined at 550 °C. In the current case overall 1.7% of Sn and 0.1% of Sr were leached to the liquid phase. The observed leaching might be a limitation for the industrial application of the Sn catalyst.

3.2.2. *Glucose transformation over Sn–Al-Beta with the addition of K_2CO_3 in the reaction mixture*

To assess the role of alkali promoters on the catalytic behaviour and their potential involvement in homogeneous reactions, glucose transformation was also investigated over Sn–Al-Beta catalyst with addition of different concentrations of K_2CO_3 into the reaction mixture. The glucose conversion after 15 min reaction time varied in the range of 96.8–99.9%, however, not showing any clear trend with K_2CO_3 concentration.

Complete glucose conversion was obtained with all K_2CO_3 amounts over Sn–Al-Beta catalyst. The total yield and carbon balance at 1440 min calculated based on the products visible in HPLC and GC analysis is given in Table 8 illustrating that the carbon balance decreased with high K_2CO_3 concentrations. It was also pointed out in Ref. [6] that alkali mediated degradation of sugars in strong alkaline solutions can occur. Glucose, fructose and methyl glucoside concentrations as a function of time are depicted in Fig. 9.

It can be seen from Fig. 9 that the rate for fructose disappearance between 15 and 45 min calculated as mmol/min/g_{cat} decreased with increasing K_2CO_3 concentration between 0.5 and 1 mM remaining constant thereafter. This result indicates that potassium neutralizes a part of acid sites, which decreased fructose transformation rate. On the other hand, an analogous trend for methyl glucoside disappearance could not be found (picture not given here).

When plotting the concentration of methyl glucoside as a function of fructose concentration it can be seen that for K_2CO_3 in the range of 0.5–1.25 mM, very low amounts of methyl glucoside were seen indicating that the added alkali salt limits methyl glucoside formation.

The influence of K_2CO_3 concentration on the methyl lactate and methyl levulinate yields after 1440 min reaction is shown in Fig. 10 and as it can be seen that both the methyl lactate and methyl levulinate yields have clear maxima as a function of K_2CO_3 concentration. At low values, the main product is methyl levulinate, while for the concentration higher than 0.5 mmol/l selectivity is shifted giving methyl lactate as the main product. The yield of methyl levulinate can be considered negligible at high concentrations of alkali when the highest methyl lactate yield of 52.8% at a 0.75 mmol/l concentration of K_2CO_3 was achieved. The current results are in line with those in Ref. [24] in which an optimum K_2CO_3 concentration was found giving ca. 22% yield of methyl lactate from xylose at 60% conversion over Sn–Al-Beta catalyst at 160 °C. Analogously an optimum amount of K_2CO_3 added into the reaction mixture containing sucrose was observed in sucrose transformation at 170 °C over Sn–Al-Beta and over Sn-MCM-41 giving methyl lactate yields of 75% and 57%, respectively [18]. In another work [43] a maximum in methyl lactate yield was obtained in sucrose transformation when using alkali-free-Sn-Beta as a catalyst and 0.03 mM K_2CO_3 as an additive in the reaction mixture at 170 °C in 16 h. This catalyst was prepared via the fluoride route reported in Ref. [44]. When further analyzing the current results, the ratio between the yield of methyl levulinate to methyl lactate vs the Brønsted to Lewis acid site ratio was plotted. It was found that this ratio between the product yields increased with increasing BAS/LAS ratio. This nicely quantifies a suggestion in Ref. [25] that methyl levulinate is formed over Brønsted acid sites [25]. An analogous trend was not, however, found in the previous series when different alkali metals were added to Sn–Al-Beta catalyst (not depicted here) indicating that the alkali metal nature has an effect on the product distribution in addition to the amounts of acid sites only. Furthermore, the total yield of all observed products decreased as follows when using different amounts of K_2CO_3: 0.065 M > 0.17 M > no K_2CO_3 > 0.75 M > 1.0 M showing that with low amounts of K_2CO_3 a higher total yield was obtained. When the total yield (right hand side y-axis in Fig. 10 b) was plotted as a function of BAS/LAS ratio (x-axis), it can be seen that higher BAS/LAS ratios are beneficial for a higher total yield in the liquid phase (>70%). Fig. 10 b also illustrates that the ratio between the yield of methyl levulinate to methyl lactate (left hand side y-axis) also increases at higher values of BAS/LAS.

Differences in methyl lactate yields can be attributed to differences in the type of acid sites and their strengths. The acid site distributions are listed in Table 3 for the experiments with different concentrations of K_2CO_3. The influence of Brønsted and Lewis acidity on the methyl lactate yield is illustrated in Fig. 11.

In these figures the quantity of weak sites W (weak) is calculated as the amount of pyridine desorbed between 250 °C and 350 °C, while medium (M) and strong (S) sites the temperature intervals were 350 °C–450 °C and above 450 °C.

Fig. 11a shows that an optimum concentration of Brønsted acid sites is required to produce a high yield of methyl lactate. This is in line with the results of [25] in which the lowest BAS/LAS ratio gave the highest methyl lactate yields in glucose transformation at 170 °C. This is valid for weak, medium and strong Brønsted acidity. On the contrary, a higher Lewis acidity promotes formation of the desired product. However, if the

Table 8
The yields of products over different catalysts at 180 °C after 1440 min in glucose transformation over Sn–Al-Beta with of K_2CO_3 into the reaction mixture. Reaction conditions: $c_{0,\ glu}$ = 5 mmol, V_L = 100 ml, m_{cat} = 0.41 g, solvent methanol, 180 °C under 30 bar total pressure under Ar.

K_2CO_3 concentration (mM)	Methyl levulinate (%)	Methyl lactate (%)	Methyl glucoside (%)	Furfural (%)	Methyl formate (%)[a]	Carbon balance (%)	Total yield of products (%)
0	31.4	19.5	0	2.5	19.5	46.0	72.9
0.065	47.2	24.9	0	4.4	18.5	66.7	95.0
0.17	36.2	28.3	0	5.6	11.4	59.0	81.5
0.5	1.9	51.4	0.4	3.2	0	38.8	56.9
0.625	1.7	52.1	0	4.3	25.7	40.0	83.8
0.75	0.7	52.8	0.7	6.3	0	41.4	60.6
1.0	0.6	36.3	0.2	6.6	5.2	30.2	48.9
1.25	0	37.8	0	7.2	25.9	30.9	70.9

[a] According to stoichiometry methyl formate should be formed in the same amounts as methyl levulinate by decomposition of HMF. Apparent fluctuations in the yield of methyl formate are related to a low boiling point of this compound. The liquid samples are withdrawn from the reactor operating at 180 °C and some methyl formate might be lost during sampling.

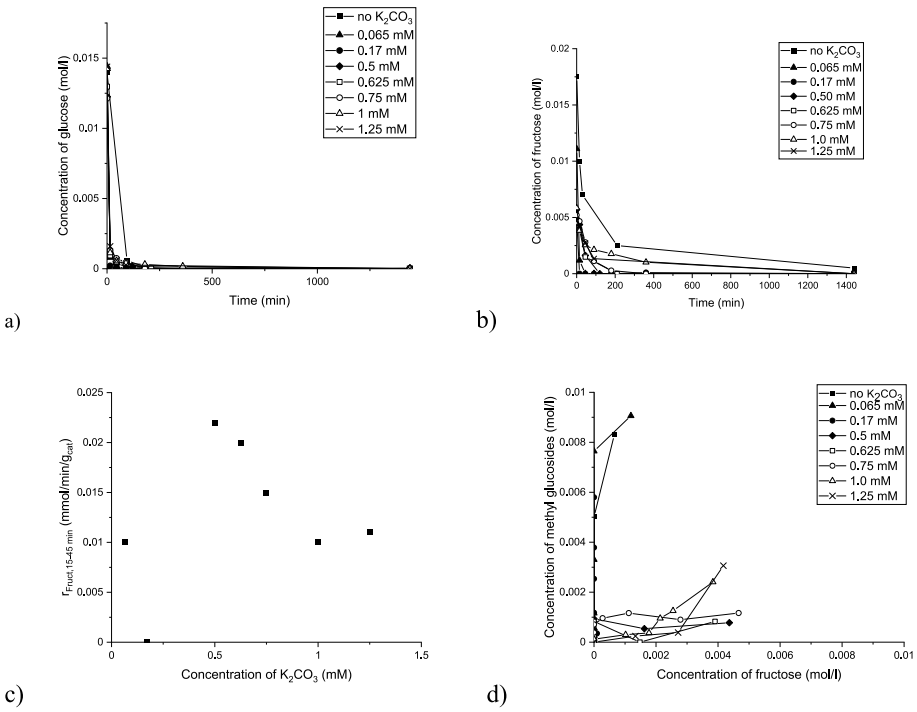

Fig. 9. Effect of K_2CO_3 addition into the reaction mixture for glucose transformation over Sn–Al-Beta. a) glucose and b) fructose concentration *vs* time, c) rate for fructose disappearance between 15 and 45 min calculated as mmol/min/g_{cat} and plotted as a function of the added amount of K_2CO_3, d) concentration of methyl glucoside as a function of fructose concentration. Reaction conditions: $c_{0,\ glu}$ = 5 mmol, V_L = 100 ml, m_{cat} = 0.41 g, solvent methanol, 180 °C under 30 bar total pressure under Ar after 1440 min.

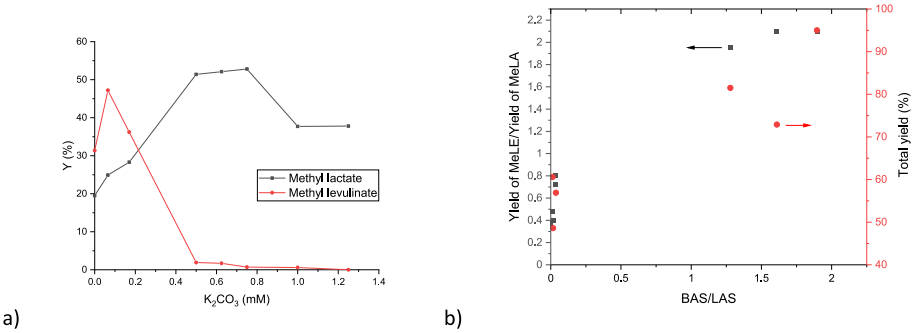

Fig. 10. a) Influence of K_2CO_3 concentration on the methyl lactate and methyl levulinate yields after 24 h at 180 °C, b) the ratio between the yield of methyl levulinate to methyl lactate as a function of the ratio Brønsted acid concentration (BAS) vs Lewis acid sites (LAS) concentration in μmol/g each. Reaction conditions: $c_{0,\ glu}$ = 5 mmol, V_L = 100 ml, m_{cat} = 0.41 g, solvent methanol, 180 °C under 30 bar total pressure under Ar after 1440 min.

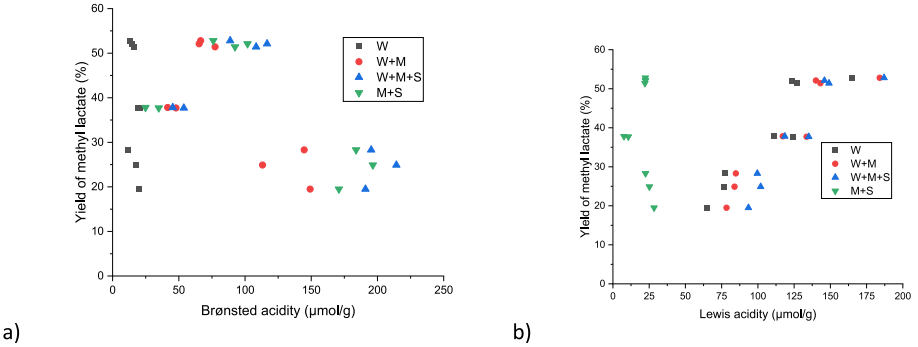

Fig. 11. Influence of a) Brønsted and b) Lewis acidity on the methyl lactate yield in glucose transformation. Reaction conditions: $c_{0,\ glu}$ = 5 mmol, V_L = 100 ml, m_{cat} = 0.41 g, solvent methanol, 180 °C under 30 bar total pressure under Ar after 1440 min. W, M and S correspond to weak, medium and strong acid sites desorbing pyridine between 250 °C and 350 °C, 350 °C and 450 °C and above 450 °C respectively.

amount of weak sites is low in comparison with the medium and strong sites a negative effect (green data points) on the yield of methyl lactate can be seen in Fig. 11b.

4. Conclusions

Sn–Al-Beta zeolite was prepared through hydrothermal synthesis and tested in catalytic transformations of glucose to methyl lactate. This material was further modified by incipient wetness impregnation with different alkali and alkaline earth metals leading to changes in acidity, in particular, the acid site distribution. The Brønsted acidity decreased in all cases while an increase in Lewis acidity was found for materials modified with calcium, magnesium and strontium, which textural properties were not affected after modifications.

The catalytic experiments were carried out at 180 °C using methanol as the solvent. It was found that the yield to methyl lactate could be improved from ca. 20% for the parent Sn–Al-Beta to the one exceeding 50% by adding promoters (especially K and Sr). It was also found that the acidic properties of the catalysts control the methyl lactate yield in a way that an optimum amount of Brønsted acidity and high Lewis acidity are beneficial for selectivity to the desired product.

CRediT authorship contribution statement

Atte Aho: Writing – original draft, Investigation. **Narendra Kumar:** Methodology, Investigation, Conceptualization. **Kari Eränen:** Methodology. **Robert Lassfolk:** Investigation. **Päivi Mäki-Arvela:** Writing – original draft, Supervision, Methodology, Conceptualization. **Tapio Salmi:** Supervision. **Markus Peurla:** Investigation. **Ilari Angervo:** Investigation. **Jukka Hietala:** Supervision, Project administration, Funding acquisition, Conceptualization. **Dmitry Yu Murzin:** Writing – review & editing, Supervision, Project administration, Funding acquisition, Conceptualization.

Declaration of competing interest

The authors declare that they have no known competing financial interests or personal relationships that could have appeared to influence the work reported in this paper.

Data availability

Data will be made available on request.

Acknowledgements

This work is part of the activities of the Johan Gadolin Process Chemistry Centre at Åbo Akademi University. Electron microscopy samples were processed and analyzed in the Electron Microscopy Laboratory, Institute of Biomedicine, University of Turku, which receives financial support from Biocenter Finland.

Appendix A. Supplementary data

Supplementary data to this article can be found online at https://doi.org/10.1016/j.micromeso.2023.112483.

References

[1] N.A.S. Din, S.J. Lim, M.Y. Maskat, S. Abd Mutalib, N.A.M. Zaini, Bioresour. Bioprocess. 8 (2021) 1–23.
[2] P. Mäki-Arvela, A. Aho, D.Yu Murzin, ChemSusChem 13 (2020) 4833–4855.
[3] M. Dusselier, P.V. Wouwe, A. Dewaele, E. Makshina, B.F. Sels, Energy Environ. Sci. 6 (2013) 1415–1442.
[4] L.S. Sharninghausen, J. Campos, M.G. Manas, R.H. Crabtree, Nat. Commun. 5 (2014) 1–9.
[5] E.A. Edreder, I.M. Mujtaba, M. Emtir, Chem. Eng. J. 172 (2011) 467–475.
[6] X.M. Yang, J.J. Bian, J.H. Huang, W.W. Xin, T.L. Lu, C. Chen, Y.L. Su, L.P. Zhou, F. Wang, J. Xu, Green Chem. 19 (2017) 692–701.
[7] X.Y. Yue, H.F. Ren, C. Wu, J. Xu, J. Li, C.L. Liu, W.S. Dong, J. Chem. Technol. Biotechnol. 96 (2021) 2238–2248.
[8] Q. Cai, X. Yue, W.S. Dong, Porous Mater 28 (2021) (2021) 1315–1324.
[9] J.M. Jimenez-Martin, A. Orozco-Saumell, H. Hernando, M. Linares, R. Mariscal, M. López Granados, A. García, J. Iglesias, ACS Sustain. Chem. Eng. 10 (2022) 8885–8896.
[10] X. Lu, L. Wang, X. Lu, Catal. Commun. 110 (2018) 23–27.
[11] X. Lyu, L. Wang, X. Chen, L. Xu, J. Wang, S. Deng, X. Lu, Ind. Eng. Chem. Res. 58 (2019) 3659–3665.
[12] X. Lyu, L. Xu, J. Wang, X. Lu, Catal. Commun. 119 (2019) 46–50.
[13] X. Zhao, T. Wen, J. Zhang, J. Ye, Z. Ma, H. Yuan, X. Ye, Y. Wang, RSC Adv. 7 (2017) 21678–21685.
[14] O. de la Iglesia, M. Sarango, M. Munárriz, M. Malankowska, A. Navajas, L. M. Gandía, J. Coronas, C. Téllez, ACS Sustain. Chem. Eng. 10 (2022) 2868–2880.
[15] L. Botti, R. Navar, S. Tolborg, J.S. Martínez-Espín, C. Hammond, ACS Sustain. Chem. Eng. 10 (2022) 4391–4403.
[16] C. Kosri, S. Kiatphuengporn, T. Butburee, S. Youngjun, S. Thongratkaew, K. Faungnawakij, C. Yimsukanan, N. Chanlek, P. Kidkhunthod, J. Wittayakun, J. Khemthong, Catal. Today 367 (2021) 205–212.
[17] T.V. dos Santos, D.O. da Silva Avelino, D.B. Pryston, M.R. Meneghetti, S. M. Meneghetti, Catal. Today 394–396 (2022) 125–132.
[18] S. Tolborg, I. Sádaba, C.M. Osmundsen, P. Fristrup, M.S. Holm, E. Taarning, ChemSusChem 8 (2015) 613–617.
[19] S. Yamaguchi, M. Yabushita, M. Kim, J. Hirayama, K. Motokura, A. Fukuoka, K. Nakajima, ACS Sustain. Chem. Eng. 6 (2018) 8113–8117.
[20] F. Wang, Y. Wen, Y. Fang, H. Ji, ChemCatChem 10 (2018) 4154–4161.
[21] R. Verma, Y.W. Insyani, S.M. Suh, S.M. Kim, S.K. Kim, J. Kim, Green Chem. 19 (2017) 1969–1982.
[22] B. Tang, S. Li, W.C. Song, E.C. Yang, X.J. Zhao, N. Guan, L. Li, ACS Sustain. Chem. Eng. 8 (2020) 3796–3808.
[23] X. Yang, Y. Liu, X. Li, J. Ren, L. Zhou, T. Lu, Y. Su, ACS Sustain. Chem. Eng. 6 (2018) 8256–8265.
[24] S.G. Elliot, S. Tolborg, R. Madsen, E. Taarning, S. Meier, ChemSusChem 11 (2018) 1198–1203.
[25] J. Iglesias, J. Moreno, G. Morales, J.A. Melero, P. Juárez, M. López-Granados, R. Mariscal, I. Martínez-Salazar, Green Chem. 21 (2019) 5876–5885.
[26] X. Yang, B. Lv, T. Lu, Y. Su, L. Zhou, Catal. Sci. Technol. 10 (2020) 700–709.
[27] B. Murillo, Ó. de la Iglesia, C. Rubio, J. Coronas, C. Téllez, Catal. Today 362 (2021) 90–96.
[28] Z. Liu, W. Li, C. Pan, P. Chen, H. Lou, X. Zheng, Catal. Commun. 15 (2011) 82–87.
[29] R.-J. van Putten, J.G.M. Winkelman, F. Keihan, J.C. van der Waal, E. de Jong, H. J. Heeres, Ind. Eng. Chem. Res. 53 (2014) 8285–8290.
[30] C.A. Emeis, J. Catal. 141 (1993) 347–354.
[31] H. Yu, F. Li, W. He, C. Song, Y. Zhang, Z. Li, H. Lin, RSC Adv. 10 (2020) 22126–22136.
[32] J.M. Newsam, M.M.J. Treacy, W.T. Koetsier, C.B. de Gruyter, Proc. Roy. Soc. Lond. A 420 (1988) 375–405.
[33] E. Yuan, W. Dai, G. Wu, N. Guan, M. Hunger, L. Li, Microporous Mesoporous Mater. 270 (2018) 265–273.
[34] Z. Yu, S. Li, A. Wang, X. Zheng, X. Jun, L. Chen, F. Deng, J. Phys. Chem. C 115 (45) (2011) 22320–22327, 115.
[35] J.P. Nogier, Y. Millot, P.P. Man, T. Shishido, M. Che, S. Dzwigaj, J. Phys. Chem. C 113 (2009) 4885–4889.
[36] X. Wang, W. Dai, G. Wu, L. Li, N. Guan, M. Hunger, Microporous Mesoporous Mater. 151 (2012) 99–106.
[37] S. Li, V.A. Tuan, J.L. Falconer, R.D. Noble, J. Membr. Sci. 191 (2001) 53–59.
[38] R. Bermejo-Deval, R. Gounder, M.E. Davis, ACS Catal. 2 (2012) 2705–2713.
[39] I. Tosi, A. Riisager, E. Taarning, P.R. Jensen, S. Meier, Catal. Sci. Technol. 8 (2018) 2137–2145.
[40] A. Aho, N. Kumar, K. Eränen, P. Mäki-Arvela, T. Salmi, M. Peurla, I. Angervo, J. Hietala, D.Yu Murzin, React. Kinet. Mech. Catal. 135 (2022) 1971–1986.
[41] A. Yamaguchi, S. Matsunaga, M. Shibasaki, J. Am. Chem. Soc. 131 (2009) 10842–10843.
[42] H. Matsuhashi, A. Iwamoto, M. Sasaki, K. Yoshida, H. Aritami, J. Jpn. Petrol. Inst. 64 (2021) 103–111.
[43] S. Tolborg, I. Sádaba, C.M. Osmundsen, P. Fristrup, M.S. Holm, E. Taarning, 1 ChemSusChem 8 (2015) 613–617.
[44] S. Valencia, A. Corma, Stannosilicte Molecular Sieved, US Patent 6306364 B1, 1999.